OFFwind Highlights No. 11 – MAY 2025

SIMULATING SEA ICE IMPACT ON A GRAVITY-BASED OFFSHORE WIND TURBINE

In regions like the Bothnian Sea and the Bay of Bothnia, significant ice cover is common. In these regions, level ice as well as pressure ridges and ice keels, thick ice formations extending below the water surface, can exert extreme loads on foundations of offshore wind turbines.

The Korsnäs wind farm, a joint venture between Vattenfall and Metsähallitus, will be Finland's first offshore wind farm in open sea, featuring 70–100 turbines with a total capacity of 1.3 GW and annual energy production of 5 TWh. This study investigates the dynamic ice–structure interaction of a 22 MW gravity-based wind turbine subjected to drifting level ice, aiming to inform the safe design of offshore wind infrastructure in ice-prone regions.

A high-fidelity numerical model is developed in LS-DYNA using a hybrid cohesive–continuum damage mechanics approach to simulate ice-induced vibrations (IIV) at varying ice drift speeds. The turbine is based on the IEA 22 MW reference design and includes detailed structural components: rotor-nacelle assembly, steel tower, and concrete gravity-based foundation (GBF).

Methods used for simulating ice-structure interaction forces on a Gravity based offshore windmill

The simulations are conducted using LS-DYNA (Release 14), employing the Cohesive Element Method (CEM) to model level ice action. The turbine model is based on the IEA 22 MW Reference Wind Turbine, featuring a 283 m rotor diameter, a hub height of 170 m, and a rotor-nacelle assembly (RNA) with a mass of 1,208 tons. The steel tower has a mass of 1,574 tons and a height of 149.3 m, starting 15 m above mean sea level (MSL). The concrete GBF, designed for 30 m water depth, weighs 6,327 tons and includes a cylindrical section, a transition zone, a conical base, and a base plate of 37.16 m diameter. The geometry and finite element model of the 22 MW gravity-based offshore wind turbine is illustrated in Figure 1.

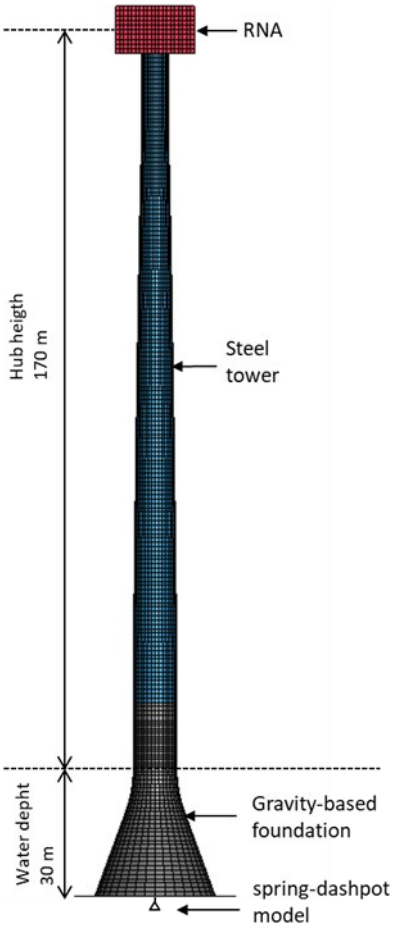

The circular foundation plate, gravity-based concrete foundation, and steel tower are modelled using shell elements. The foundation diameter at the waterline is 10.0 m. A classical soil-structure interaction model (spring-dashpot) is used, representing medium dense moraine. The rotor-nacelle assembly (RNA) is modelled with volume elements using a smeared mass approximation, where total mass is uniformly distributed over a simplified bounding box. Density is adjusted to preserve correct mass and dynamic response. This approach reduces computational cost while maintaining realistic dynamic behavior and is commonly applied when detailed RNA modelling is unnecessary.

Figure 1. Geometry and finite element model of the 22 MW gravity-based offshore wind turbine.

Modelling of ice-structure interaction

To be able to represent the behaviour of ice over a broad range of strain rates, elastic, time-dependent (creep) and instantaneous, inelastic components of deformation must be considered. The resulting constitutive model is commonly referred to as a visco-plastic formulation. Here, only the instantaneous, inelastic part is considered, and it is interpreted based on the theory of plasticity. In this study, it is assumed that the ice behaves as an elasto-plastic continuum that can fracture. The ice sheet is modelled using hexahedral elements (bulk elements) with elastic-plastic, transversally isotropic material properties using Hills yield criterion combined with isotropic damage to take account for softening in the compressive regime. Each individual bulk element is joined to its neighbours using so called cohesive elements, which are the potential crack planes to simulate the crack initiation and growth of ice as shown in Figure 2. To account for the anisotropic behaviour and fracture of columnar ice, different cohesive properties are given for cohesive elements with faces normal to the X-, Y- and Z-axes as shown in Figure 2.

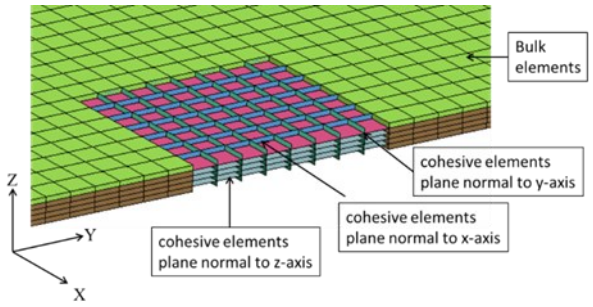

Figure 2. Illustration of the ice sheet mesh topology.

The cohesive element represents the cohesive force while following the traction-separation curve. A cohesive constitutive law relates the traction, force per unit area, to the separation at the interface via non-linear spring elements. The separation between adjacent bulk element surfaces when subjected to tension or shear responds by deforming according to a given traction-separation curve are derived based on the displacement at Gauss points in the cohesive elements. When the force or deformation reaches a limit value the cohesive element is eroded and thus a crack is formed, and a fracture energy is dissipated. A crack can grow by the deformation and failure of neighbouring cohesive elements. Contact conditions are added to all faces of the bulk elements so that friction can occur if sliding occurs in a closed crack. It follows that for a sufficiently large deformation of the ice sheet, regions where cohesive elements erode, are reduced to ice rubble, i.e. the bulk elements interacting only by contact and friction and developing a frictional ice mass.

Geometry and Lagrange element mesh of the ice sheet and gravity-based foundation is shown in Figure 3. The ice sheet is modelled with length L= 70 m and width W=40 m. The boundary conditions of the edge ABCD were such as to keep the ice sheet in a horizontal position and fixed in global Z- and Y-direction. The edge AD is free. An initial ice speed is prescribed for the entire ice sheet, and the movement of the ice sheet is controlled by specifying an ice speed along boundaries ABCD in global X-direction for the simulated load scenario. The 50-year extreme ice thickness is 0.77 m obtained for Korsnäs wind farm area and used in the simulations of ice-structure interaction process. A purpose-built mesh generator is used for generating the finite element mesh consisting of bulk- and cohesive elements and springs-dashpot system to account for buoyancy forces acting on the ice. This mesh generator calculates the interconnectivity between bulk- and cohesive elements, as well as the elasto-plastic material properties of bulk elements.

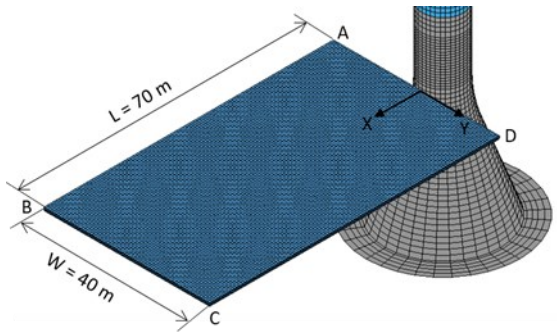

Figure 3. Geometry and Lagrange element mesh of the ice sheet and gravity-based foundation.

Two types of penalty contact formulations were defined which are between ice and structure and ice block-to ice-block contact. Eroding surface-to-surface contact is used between the ice sheet and the GBF with and the dynamic friction is 0.05 and static friction 0.1. The ice block-to-ice block friction model mimics sea ice to sea ice friction with static friction coefficient 0.57 and dynamic friction coefficient of 0.06.

FE-modelling of fluid-structure interaction

The Arbitrary Lagrangian–Eulerian (ALE) method is currently the most widely employed technique for simulating fluid–structure interaction (FSI), as it enables explicit modelling of the coupled interaction between fluids and structural components. In this framework, a Lagrangian formulation is applied to structural materials, while an ALE formulation is used for modelling the fluid domains, specifically water and air. Coupling between the fluids and structural components is achieved using a contact-type algorithm that transfers forces and motion across the fluid–structure interface.

Figure 4 presents the fluid–structure interaction (FSI) model capturing the coupled response between sea ice and a gravity-based offshore wind turbine (GBF). The model integrates the fluid domain, comprising water and air, with the FE model of the ice–structure interaction framework depicted in Figure 3. Both fluid phases are discretized using eight-node hexahedral elements and simulated with a one-point ALE multi-material formulation, allowing for interface tracking between air and water within shared elements.

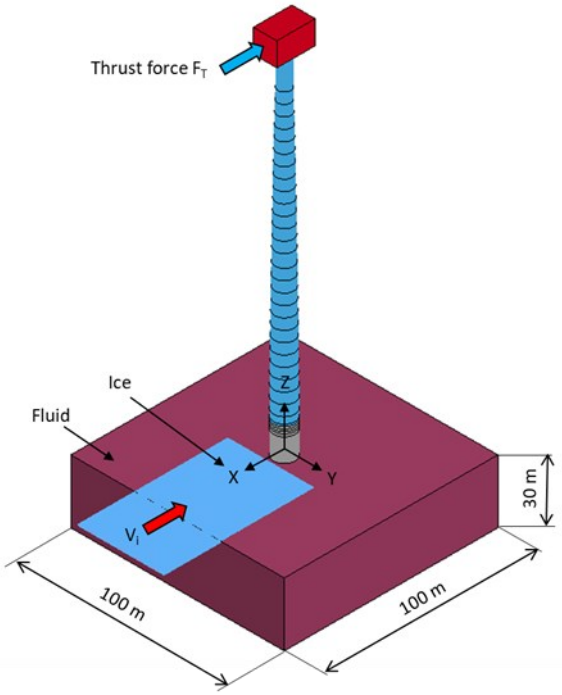

Figure 4. Sea ice and the OWT interaction model with fluid-structure interaction coupling.

The computational water domain extends 100 m × 100 m horizontally with a depth of 30 m and is meshed using 2 m × 2 m × 2 m elements. Water is modelled using so called null materials, characterized by its density, viscosity combined with Grüneisen equation of state parameters. An overlying 10.8 m thick air layer is included to ensure a free surface boundary for the water; it is also meshed using brick elements (not shown in Figure 4). For computational efficiency, the air phase is approximated as a vacuum, using only its density. The water–structure interaction is resolved by combining the ALE-formulated fluid domains with the Lagrangian structural components through a penalty-based contact algorithm, enabling effective FSI coupling within the simulation.

Thrust force is the primary aerodynamic load acting on offshore wind turbines (OWTs) during operation, critically affecting the structural design of the tower, nacelle, and foundation. In this study, the aerodynamic loading is idealized by excluding explicit rotor blade modelling; instead, the total thrust is applied as a point load at the rotor hub centre, aligned with the rotor plane (see Figure 4). This simplification effectively captures the global aerodynamic response while minimizing computational demand, assuming a steady, uniform wind field. For the IEA 22 MW reference wind turbine (RWT), the thrust force exhibits minimal variation within the 9.0–11.8 m/s wind speed interval, peaking at 2.66 MN.

Numerical simulation setup and results

The time series of global ice forces acting on the gravity-based concrete foundation of the wind turbine are plotted in Figure 5 for ice thickness 0.77 m and ice speed of 0.25 m/s. The global ice forces F_X, F_Y, and F_Z acting along the X-, Y- and Z- directions respectively, are illustrated in Figure 4. The numerical simulation is terminated after 40 s and the GBF has penetrated 10 m into the ice sheet. Maximum global ice force F_X = 9.47 MN occurs at 36.9 s, with an average of 3.54 MN. Figure 5 also shows that the global force F_Y, acting normal to the ice drift direction, is not symmetric around the periphery of the gravity-based foundation. The global force F_Y fluctuates between a minimum value of -2.6 MN at 16.7 seconds and a maximum value of 3.1 MN at 21.0 seconds. The global vertical force F_Z fluctuates between a minimum of -0.67 MN at 19.4 seconds and a maximum of 0.57 MN at 37.2 seconds. In this case, mechanical properties of the ice sheet were characterized by a uniaxial compressive strength of 3.7 MPa in the horizontal direction and 6.7 MPa in the vertical direction.

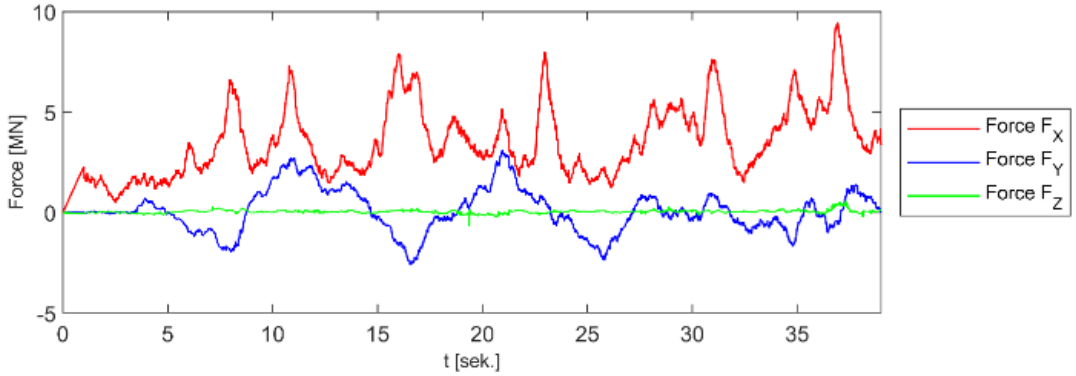

Figure 5. Time series of global ice forces obtained by numerical simulation for ice thickness 0.77 m and ice speed 0.25 m/s.

The corresponding tensile strengths were 0.63 MPa and 1.65 MPa in the horizontal and vertical directions, respectively.

Summary and conclusion

Numerical simulations were conducted for ice drift speeds ranging from 0.05 to 0.55 m/s, with a constant ice sheet thickness equal to 0.77. Key level ice properties, including uniaxial compressive and tensile strengths, were varied to reflect rate-dependent behavior. The simulations model ice-structure interaction with a gravity-based foundation (GBF), accounting for local failure modes and dynamic effects.

Ice Load Characteristics:

- Peak horizontal ice forces reached up to 9.47 MN (at 0.25 m/s), corresponding to 76–94% of the global force (10.08 MN) estimated according to ISO 19906:2019 (Petroleum and natural gas industries - Arctic offshore structures)
- Mean ice force increased with drift speed, reflecting intensified sustained loading.
- Average-to-peak force ratios rose from 0.36 to 0.58 across the drift speed range, indicating more dynamic engagement at higher velocities.

Frequency Response Analysis:

- At the waterline, dominant acceleration frequencies ranged from 11.8 to 47.9 Hz, i.e. medium/high frequencies, highlighting local dynamic ice-structure interactions.
- At the nacelle, dominant acceleration frequencies were consistent across drift speeds (0.14 Hz, 0.47 Hz, and 1.48 Hz).
- The 0.14 Hz mode lies below the dry natural frequencies of the Gravity based offshore windmill (0.152–0.153 Hz) but overlaps with the blade passing frequency band (P3: 0.099–0.358 Hz), suggesting potential for dynamic coupling with rotor-induced loads.

The observed frequency overlap indicates risk of frequency lock-in and multi-frequency resonance, potentially amplifying fatigue demands in critical components due to combined effects of ice and aerodynamic excitation.

AUTHOR:

Bjørnar Sand

Senior Research Scientist

SINTEF Narvik AS, Narvik, Norway

Email: bjornar.sand@sintef.no

Interreg Aurora

Co-funded by the European Union

LAPIN LIITTO

MERINOVA TECHNOLOGY CENTRE

LULEÅ UNIVERSITY OF TECHNOLOGY

NOVIA UNIVERSITY OF APPLIED SCIENCES

Tampere University

SINTEF